

# A contractor muscle based continuum trunk robot

Alan Bartow, Apoorva Kapadia, and Ian D. Walker

**Abstract**— We present a new and novel continuum robot, built from contracting pneumatic muscles. The robot has a continuous compliant backbone, achieved via three independently controlled serially connected three degree of freedom sections, for a total of nine degrees of freedom. We detail the design, construction, and initial testing of the robot. The use of contracting muscles, in contrast to previous comparable designs featuring expanding muscles, is well-suited to use of the robot as an active hook in dynamic manipulation tasks. We describe experiments using the robot in this novel manipulation mode.

**Keywords**—robotics, continuum, trunk, tentacle.

## I. INTRODUCTION

Traditional robot manipulators, based on rigid-link structures, are at this point in time a mature and well-understood technology. The inherent rigidity of their structure provides high precision and repeatability, and enables their core industrial applications of parts handling and assembly. However, the very rigidity of the links makes it difficult or impossible for traditional manipulators to adapt their shape sufficiently to operate within cluttered environments. In addition, their inherent rigidity makes it difficult to deploy traditional robots in more unstructured, “real-world” applications where (a priori unplanned) physical interaction with the environment is crucial.

In response to the above limitations of traditional robot manipulators, in recent years researchers have been investigating continuous backbone, or continuum, robots [18], [20], [23]. Inspired in large part by biological “tongues, trunks, and tentacles” [12], researchers have developed continuum robots emulating key features of elephant trunks [4], [7], [21] and octopus arms [6], [14], [22].

Ian Walker is with the Department of Electrical and Computer Engineering, Clemson University, Clemson SC 29634 USA (corresponding author, phone: 864-656-7209; fax: 864-656-7220; e-mail: iwalker@clemson.edu).

Alan Bartow is with the Department of Electrical and Computer Engineering, Clemson University, Clemson SC 29634 USA (e-mail: abartow@clemson.edu).

Apoorva Kapadia is with the Department of Electrical and Computer Engineering, Clemson University, Clemson SC 29634 USA (e-mail: akapadi@clemson.edu).

This research was supported in part by the U.S. National Science Foundation under grant IIS-0904116, and in part by NASA under contract NNX12AM01G.

Continuum robots are not only able to bend and at any point along their backbone, they also exhibit significant compliance [20], [23]. These capabilities offer the potential for “snake-like” exploration of congested environments [8] and adaptive “whole-arm” grasping (using any part of the robot, not just an end effector at the tip) of arbitrarily shaped objects [16]. Potential applications include numerous medical applications [23], [24], search and rescue operations [21], applications within airframes and nuclear reactors [3], and underwater operation [1], [13] as well as provably safe health care robotics in congested patient rooms [2], [25].

A common design strategy well suited for continuum robots is the incorporation of pneumatic actuation [20], [23]. Pneumatics has the advantage of both being inherently compliant due to the compressibility of air [10]. Pneumatic actuation of continuum robot structures have been achieved via pressurization of specialized chambers [9], [15], [19]. However, a more common strategy is to use artificial air (“McKibben”) muscles [5], [6], [14], [16], [17]. Continuum robot backbones can be built from pneumatic muscles, with their supply tubing routed within the structure. The backbone can be conveniently created as a series of “sections”, each section made from a set of (typically three) pneumatic muscles connected in parallel. Each section can be made to bend in two dimensions, and also extend or contract, by controlling the differential pressure in its constituent muscles.

Pneumatic muscle hardware can be built as extensors (increasing length with increase in pressure) or contractors (decreasing length with increase in pressure). While the contracting type is analogous to the operational mode of human muscle, continuum robot hardware and analysis in the literature has thus far concentrated on extensible actuators [11], [20], [23]. This choice is motivated in part by the notion of backbone extension into complex environments. However, the potential and possible novel capabilities offered by backbones actuated by contractor muscles have been largely neglected in the literature.

In this paper, we present a new and unique continuum robot trunk actuated entirely by contractor muscles. The robot is demonstrated to have novel and advantageous capabilities compared with existing extensor-actuator based continuum robots. The following section describes the design methodology and construction details for the robot. Operation and experiments with the prototype are discussed in sections III and IV. Conclusions are presented in section V.

## II. ROBOT DESIGN AND CONSTRUCTION

The high level design goal for the new robot was to create a contractor-actuated continuum robot with the same workspace as the successful series of octopus arm inspired “Octarm” robots ([14], [16] Fig. 1). The Octarm continuum robots were actuated by extensor pneumatic muscles [16]. A key goal was to evaluate the capabilities of the new contractor-based robot in comparison to those of the earlier extensor-based Octarm robots.

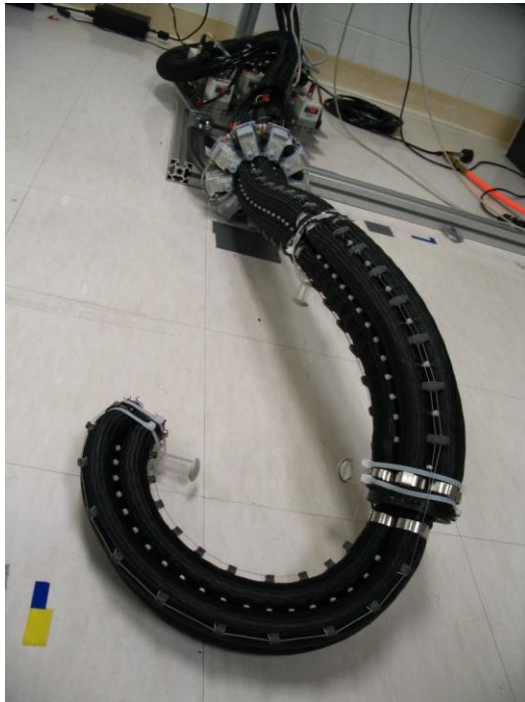


**Figure 1.** Octarm continuum manipulator.

The Octarm robots feature three independently actuated sections, for a total of nine controllable degrees of freedom. Each section is actuated by three independently controlled pneumatic pressures, fed into extensor muscles. The unpressurized robot is therefore at its minimum length, and extends to its maximum length as a function of active actuation.

The new robot was correspondingly also designed to have nine degrees of freedom, achieved via three sections each of three degrees of freedom. Due to the use of contractor muscles however, the at-rest (unactuated) length of the new robot is necessarily its maximum length, with the length contracting as a function of actuation. Therefore the nominal unactuated lengths of the sections (unactuated length of the muscles which comprise them) were selected to be the maximum lengths of each of the corresponding Octarm sections. The design goal was to achieve the same range of section lengths and curvatures as in the Octarm (Table 1). The overall muscle arrangement within the structure, and the muscle (and hence arm) diameters were specified to be approximately the same as the Octarm.

Section	Max Length	Min Length	Max Curvature
1	0.46 m	0.325 m	9.09 m <sup>-1</sup>
2	0.47 m	0.32 m	9.09 m <sup>-1</sup>
3	0.55 m	0.38 m	11.11 m <sup>-1</sup>

**Table 1.** Octarm individual section properties.

Given the desired rest length and diameter, each muscle was constructed from its individual components in our laboratory. Latex inner tubes were inserted within braided nylon mesh and capped at each end. One end cap was sealed, with the other cap containing a connection for an input tube. The braid was clamped to the tubes at the ends to complete the construction of the pneumatic actuator.

The key factor determining whether a pneumatic actuator of this design type is an extensor or contractor is the (predetermined) angle between the braids of the constraining nylon mesh. As pressure in the inner tube is increased, the braid angle determines whether the diameter can increase, with the overall muscle shortening (i.e. a contractor), or whether the length of the muscle can increase, with the diameter decreasing (i.e. an extensor). Extension occurs for braid angles less than 54.7 degrees, and contraction for braid with an angle greater than 54.7 degrees. Interestingly, a parallel phenomenon is observed (with the same critical angle) in the functionality and angles between fiber angles muscles in a variety of natural pneumatically actuated structures [12]. For the new robot actuators, a braid was selected to create contractors.

Once the muscles were manufactured, they were grouped together to form the sections of the new robot. This was achieved by fixing them, in sets of three, together into the sections by threading plastic zip ties at regular intervals through the braids of sets of three muscles along their length (Fig. 2). This constrains the section to bend evenly as a function of differential pressure in the individual muscles, but also allows the overall length to change as a function of overall pressure.



**Figure 2.** Three muscles connected by zip ties at regular intervals to form a section.

The three sections next needed to be integrated together in series to complete the construction of the robot. This required the design and manufacture of several special purpose plates and manifolds, in order to route the supply tubing for the distal section internally through the proximal ones. This was desired in order to have a smooth arm surface, with no external tubing. The required manifolds (Fig. 3) were designed in Autocad and machined from Delrin, a light but durable material. The connection procedure is indicated Fig. 4.

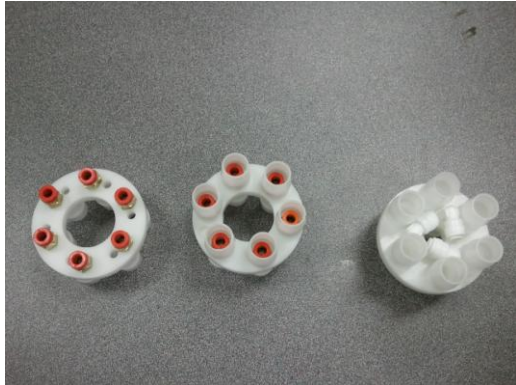


**Figure 3.** Manifolds for internal routing of pneumatic supply hoses.

The manifolds were fitted with standard pneumatic fittings (Fig. 3), with the connections sealed to ensure against leaks. The input air supply tubes were connected to these fittings (Fig. 4), with the muscle body ends clamped onto protrusions specifically designed for this purpose using hose clamps (Fig. 4).



**Figure 4.** Internal air supply hose connections using manifolds.

Finally, the robot was carefully assembled, pressurized and tested (Fig. 5). Some minor air leaks necessitated the tightening and re-sealing of some connections, but beyond that the robot was ready for testing and operation. It was mounted on an aluminium frame base (Fig. 5), with the air supply cables (top left, Fig. 5) routed to a custom-built module containing the nine pressure regulators providing the controllable input supply. The modular base allowed easy remounting from vertical to horizontal operation.



**Figure 5.** Fully assembled robot.

### III. OPERATION

The first experiments with the new robot consisted of pressurizing each section independently, to measure and evaluate their properties and capabilities. Table 2 shows the measured extension and bending capabilities of each section. The extension properties, though lower in range, matched reasonably well the corresponding properties of the extensor-based Octarm, validating the achievement of the basic design goals. However, the curvatures achieved were significantly lower than with the extensor Octarm sections. In subsequent experiments, we have found that pre-stretching the nylon mesh can produce significantly higher performance in these contractor actuators. Therefore in future similar designs, it can be expected that significantly greater curvatures can be achieved.

Section	Max Length	Min Length	Max Curvature
1	0.44 m	0.40 m	2.72 m <sup>-1</sup>
2	0.47 m	0.41 m	2.74 m <sup>-1</sup>
3	0.57 m	0.50 m	3.42 m <sup>-1</sup>

**Table 2.** New robot individual section properties.

In order to obtain coordinated motion of the overall robot, empirical work to determine appropriate control gains was conducted. The supply and control system used for the robot was the same one used for the Octarm robots [16]. This system uses as its core control element a commercial portable air pressure regulator. The supply from this is fed to nine commercial pressure regulators, which independently control the pressure supply to the individual muscles (in the range 0 to 60 psi).

The regulators, which are voltage (i.e. analog) controlled, are commanded from a standard PC via Matlab/Simulink and a commercial Quanser hardware interface board. The PC also contains software for motion planning and shape sensor-based control for continuum robots, but this was not used in the experiments reported herein.

In order to successfully operate the robot, a strategy for describing the desired shape and relating it to the controllable inputs was necessary. For continuum robots, this is a more complicated procedure than for conventional rigid-link robots, where for example, kinematics relating motor shaft angles to joint angles and hence (directly) robot configuration can be used. Continuum robots have, in theory, an infinite number of degrees of freedom, but only a finite number of actuators. This places them in the general class of underactuated robots [20], [28]. For such underactuated robots, a strategy to relate input values to robot configuration is a key requirement.

Fortunately, most continuum robots exhibit the simplifying property that each of their sections has approximately constant curvature [23], [28]. This (artifact of logical design) is due to internal energy producing evenly distributed internal forces throughout the section. In the case of pneumatically actuated sections, the air pressure acts evenly within the bladders of the actuators, subject to the differential pressures in the three section actuators, to produce consistent bending, and thus constant curvature. See Fig. 6 for an example of this for one of the contractor sections of the new robot.



**Figure 6.** Section of new continuum robot demonstrating the constant curvature property.

The constant curvature property reveals the underlying physical constraint that the shapes of continuum robot must be segments of circles, spatially connected together in series. Both the lengths and curvatures of the circle segments are variable. Note that constant curvature implies that each section lies in its own plane. However, at the intersection of two sections, the more distal section can be rotated about their common tangent, to produce a spatial general configuration.

Therefore, the shape of each section, and ultimately the entire robot, can be fairly simply modeled, given three values per section: length, section curvature, and orientation (essentially, angle of the plane the section is in, relative to the previous section). There are the core configuration space variables for continuum robots [28].

Using simple geometry, kinematic models can be formulated ([23], [28]) which relate the configuration space variables to task space (i.e. end effector or tip) variables,

similar to the procedure for conventional rigid-link robots. However, unlike the case for conventional robots, the relationship between the configuration space and actuator space variables is typically fairly complex. In the case of sections built from three coupled compliant elements the actuator inputs (air pressure as considered here) basically control three lengths, with the robot shape the results of coupling of these lengths.

Transformations between the lengths of the actuators and the configuration space variables are therefore required in order to achieve a given robot shape with the available inputs. A general set of such transformations have been developed in [23].

Therefore, for inputting desired shape information to the new continuum robot, a control system was designed in Simulink that reflected the constant curvature nature of the sections, and the need to convert between them and input actuator lengths. This system took as input three values: length, curvature, and orientation direction (termed  $\phi$ ) for each of the three sections. For each of the sections the input data was converted to desired lengths of each of the three muscles in the section using kinematics previously derived for this type of three degree of freedom curved section [20], [23]. These muscle length values were then converted to pressure regulator gain values through new models developed as discussed in the following paragraph.

The equations to determine pressure regulator gain value from muscle length was derived empirically. The length of the muscles was measured and recorded at 6 discrete input gain values of 0 through 5. Each discrete jump in gain value resulted in a 13 psi increase in air pressure delivered to each muscle. 65 psi, or a gain value of 5, was found to be the maximum allowable pressure available to the system before safety and damage to the robot were compromised. Using the recorded lengths corresponding to the gain values a linear trend line was found. This procedure was repeated for each muscle on all three sections.

These gains were then output to the air pressure regulators. In order to ensure that the system did not output pressures beyond the allowable pressures of the system, 0 to 65 psi, limits were placed in several cases. The first limits were placed on the input values of the section length and curvature that are shown in Table 2. This was done to prevent an input that was physically impossible for the robot.

A second set of limits was imposed before the gains were sent to the air pressure regulators: these did not allow the outputs to be less than 0 or greater than 5. This was done in case a combination of section length and curvatures were within the theoretical limits but not physically possible, such as requiring the maximum length and the maximum curvature both at the same time. (Lengths and curvatures in variable length continuum sections are coupled, with maximum curvatures achievable at specific – not necessarily maximum – actuator lengths.)

Another safety measure implemented was to create a complete replica control system that was completely simulated. This allowed us to test shapes and trajectories to confirm that they were acceptable for the real system to implement. If the simulation output were predicted by the

simulation to be within the gain limits, the shape or trajectories could be used safely.

#### IV. EXPERIMENTS

We conducted a variety of experiments testing the robot's ability [26]. Whole arm grasping with the robot was achieved (Figs. 7-9). However, the relatively low achievable curvatures (compared to the Octarm) meant that the range of graspable objects was limited to relatively large sizes of objects, of the general scale of its section lengths.

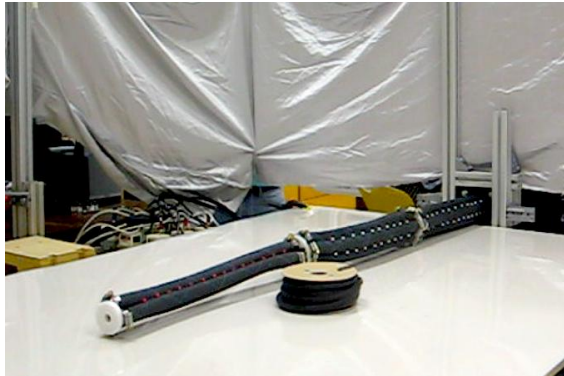


**Figure 7.** Whole arm grasp of cable reel: initial configuration

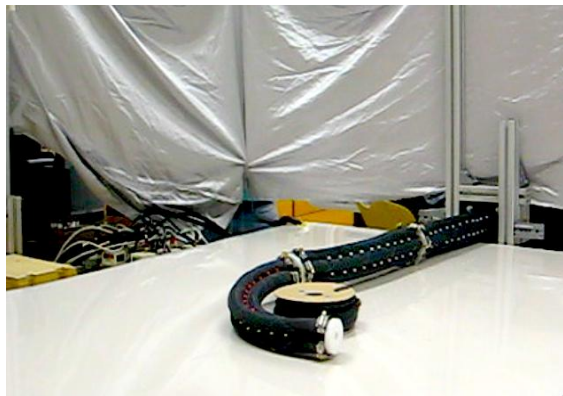


**Figure 8.** Whole arm grasp of cable reel: intermediate configuration

The new contracting robot was able to use its backbone maneuverability to successfully negotiate obstacle fields. However, the contractor muscles presented some disadvantages when entering such fields. Typically, human operators and algorithms anticipate continuum robots extending to “snake into” and around obstacles. The extensor-based Octarm, which when unpressurized is at its minimum length, is well-matched for this, beginning extension at low actuator pressure levels.

However, while the new robot can also both extend and contract, it requires maximum actuator pressure to be at minimum length, which means to extend into an obstacle field, it must first be given high actuator inputs to shrink before expanding as those input values are reduced. This was somewhat counterintuitive for the operators. Of course the opposite phenomenon is true for reducing length to exit

obstacle fields, where the contracting robot has the inherent advantage.

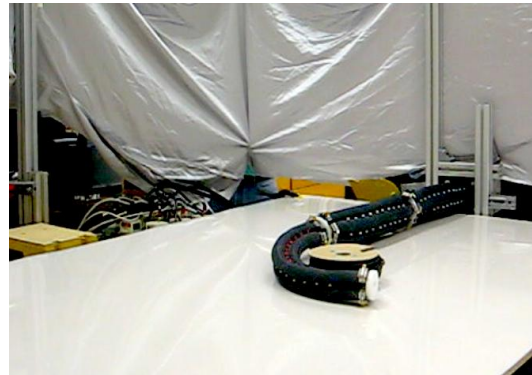


**Figure 9.** Whole arm grasp of cable reel: grasp acquired

Overall, the new robot was adequate, but not superior to the comparable extensor-based Octarm robots in whole-arm manipulation and obstacle avoidance. These have been the two most explored uses for continuum robots to date, and our results do not suggest that contractor-based robots like the one introduced in this paper are likely to be preferable in these domains, for the reasons detailed above.

Where the new robot presented the biggest advantage however was in its use as a “tunable hook”. By shaping the trunk into a variety of hook-like shapes, it was possible to successfully pick up a variety of objects with “holes and handles”, for example the headphones shown in Fig. 10. This task was found to be particularly straightforward for the new robot as compared with the extensible Octarm, which would require more complex motion in order to perform the same task.

One example of this straightforward characteristic is demonstrated in a series of experiments completed where an object to one side of the robot in a plane is hooked, grasped, and moved. In these experiments the contracting Octarm was placed horizontally on a plane with an object at its side. The arm was given a reference shape that hooked the object, and then given another reference shape that pulled the object towards its base. An extensible section-based Octarm would have to first extend itself, create the hook shape, and then contract itself. This procedure modifies section length, a time consuming step, to a simple task, using the new contractor-based robot.

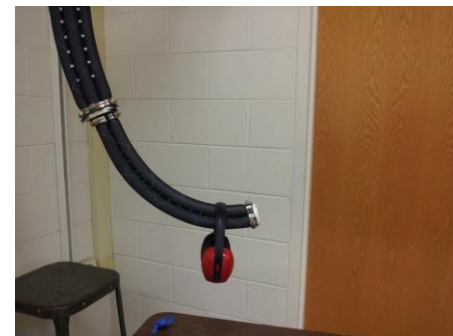


**Figure 10.** Hook grasp of headphones

In addition to hook grasping, the robot proved adept at maneuvering objects along the backbone, adaptively “flipping and throwing” them into desired locations (boxes and bins). In order to show this several experiments were created, these experiments varying in degrees of difficulty.



**Figure 11.** Configuration for “flip and throw” experiment with headphones

The first experiment created was a simple task of lifting a pair of headphones, as shown in Fig. 11, and then dropping them into a box. In this experiment the contracting Octarm is free to move in all three directions in open space. This task was done by creating a shape that interleaves the tip of the Octarm through the spine of the headphones. The next shape given was one that lifted the arm. The implemented lift of the arm is not drastic because of the gravitational forces that diminish the effectiveness of the arm in this configuration; however the lift was significant enough to pick up the headphones.

After being lifted, the arm was given a reference shape to move the headphones in a horizontal direction. This was done by changing the phi value, while holding the section length and curvature values constant. This essentially rotates the direction the arm points in without changing the shape. The final configuration had the Octarm go back to its original straight shape in order to drop the headphones into the box.

The experiment was run in a way that the Octarm went through the shapes in discrete intervals, instead of using smooth transitions. This caused accuracy problems because of the fast movements at the transitions. In order to correct this in the next experiment the shapes were given transitional input values between two points in order to create a smooth movement.

Another experiment created to show the hook grasping capabilities had the contracting Octarm lift a baseball cap off of a stand and then move it into a box. This was done while the Octarm was initially lying down in a horizontal plane (Fig. 12). This gave the robot limited directional movement, but also lessened the sagging of the robot due to gravitational forces.

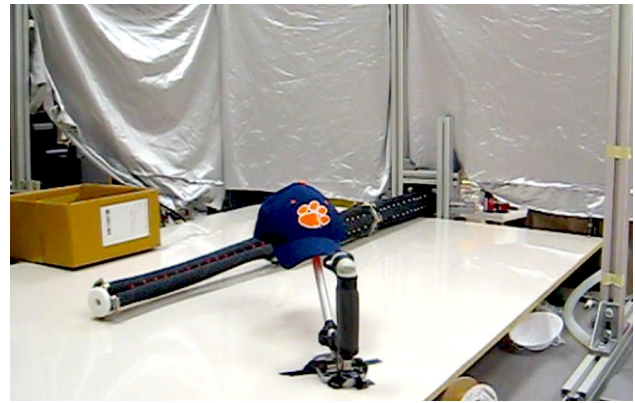


**Figure 12.** Grasp of floppy hat: initial configuration with robot in horizontal plane

This motion had five main reference postures that made up the shapes. The first reference shape consisted of placing the tip of the Octarm in the opening of the baseball cap. The main obstacle in creating this posture was avoiding knocking the hat off the stand. The next reference shape created was the act of lifting the baseball hat off of the stand. This posture’s difficulty came in keeping the hat from getting caught on the stand. To avoid this, the lifting posture also pulled the hat slightly towards the base, farther from the tip of the stand (Fig. 13).

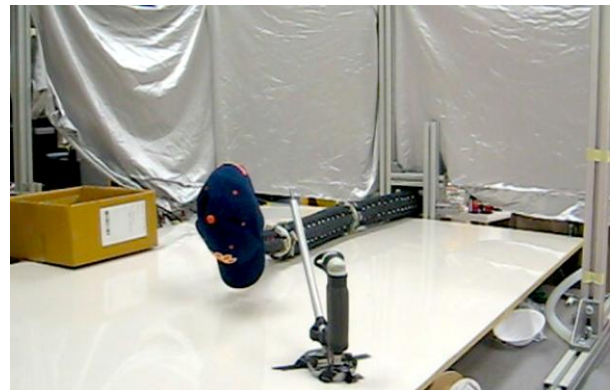


**Figure 13.** Grasp of floppy hat: initial grasp

The third reference shape was created to start the movement of the hat to the box. The box was placed on the opposite side of the Octarm as the hat stand; this meant the arm had to swing across its main axis to place the hat. The third reference shape featured the Octarm, with the hat on the tip, curled up pointing along its axis. This was done to keep the hat from falling off in transition, and because it provided a good halfway point check (Fig. 14).

The fourth, and most difficult to determine, reference shape placed the tip of the Octarm over the box where the hat was dropped. This was a difficult shape to synthesize because it had to be in such a position that it dropped the hat into the box at this point. If the hat was still on the Octarm at this point, it would not have consistently fallen off when the Octarm was retracted from over the edge of the box. In order to achieve this, the tip had to be positioned over the box and pointing towards the bottom. This causes the baseball hat to slide off the end of the tip and into the box. The final shape

that is inputted is the starting position in order to get the Octarm out of the box (Fig. 15).

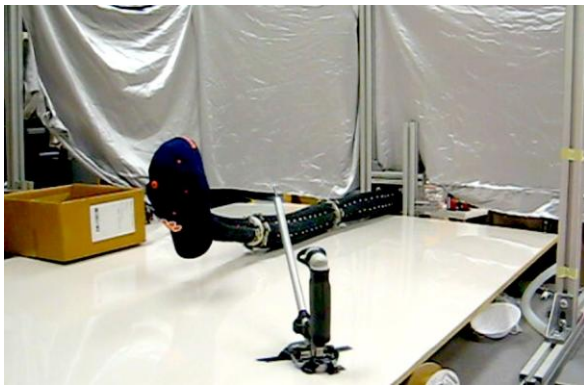


**Figure 14.** Grasp of floppy hat: intermediate grasp

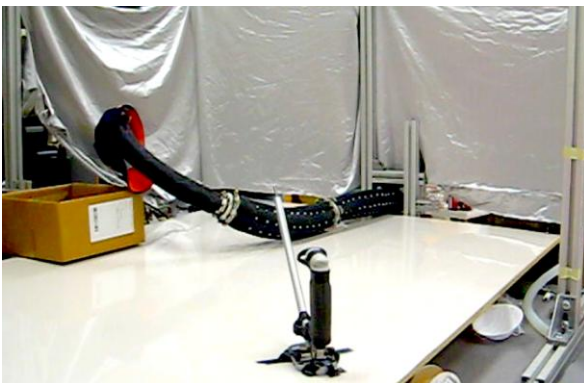


**Figure 15.** Grasp of floppy hat: grasp over box

The main difficulties of this experiment were creating postures that were repeatable, and did not allow the robot to drop the hat during pickup or movement. These issues were resolved by the trajectory synthesized. As noted before, intermediate trajectory shapes were made by interpolating the section lengths and curvature between the main postures. This provided a smooth trajectory that moved from posture to posture, and consistently doing so throughout the trajectory. This meant the robot moved to the same posture trial after trial.

A further experiment featuring the robot in direct human interaction was conducted. Placed horizontally on a table, so that its mid-section rested on the table, the robot was located opposite to a human participant (Fig. 16).



**Figure 16.** Initial human-interaction configuration

The human put his elbow on the table, and grasped the robot tip section (Fig. 17).

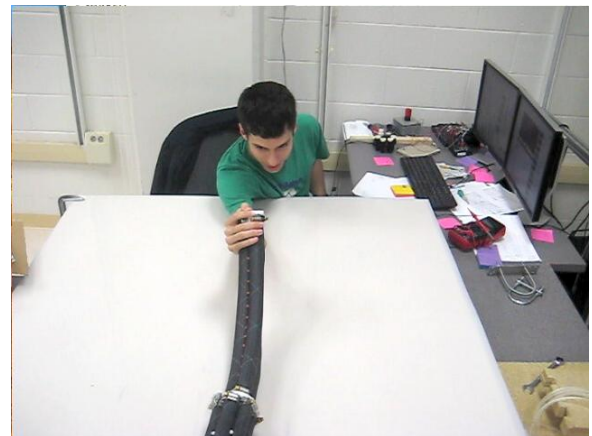


**Figure 17.** Arm wrestling configuration

The robot motion was commanded so that the human/robot pair “arm-wrestled” until either the human wrist or robot tip section touched the table (Fig 18). The robot proved the winner (Fig. 19). This experiment, which whimsical, successfully demonstrated the use of the compliance of the robot, and the inherent safety of its interactions with humans.



**Figure 18.** Arm wrestling – intermediate configuration



**Figure 19.** Ultimate arm wrestling configuration

The above forms of novel dynamic grasping and throwing manipulation make good use of the compliant and smooth backbone form, and were very easy to achieve with the new contractor-based robot. This suggests that this type of continuum robot could be well-matched to novel dynamic manipulation tasks.

## V. CONCLUSIONS

We have described the design and operation of a new and novel continuum trunk robot manipulator. The robot has nine degrees of freedom, in the form of three independently controlled serially connected sections, each with three degrees of freedom. Each section is formed from pneumatic actuators, and can bend in two dimensions as well as expand and contract in length.

The key innovation in the design is the use of contractor pneumatic artificial muscles as the actuators, whereas previous variable length continuum robots have used extensor actuators. The contractor muscles reduce in length as pressure increases. Thus the unpressurized robot is at its maximum length, and contracts during operation. This feature leads to new and sometimes unexpected operational modes, when used for grasping and manipulation.

Experiments conducted with the new robot showed that while the contractor trunk could whole-arm grasp large objects and navigate complex obstacle fields, it is not superior to comparable previous extensor-based continuum robots in this regard. The new robot is however significantly more adept at “adaptive hooking” than comparable extensible muscle-based Octarm designs. This suggests that continuum robots based on contractor muscles could be particularly useful in use as active hooks.

Our ongoing and future efforts center on novel adaptive and dynamic manipulation experiments with the new trunk robot. In particular, we are investigating the ability of the design to support novel impulsive manipulation.

## REFERENCES

- [1] V. C. Anderson and R. C. Horn, Tensor Arm Manipulator Design, *Transactions of the ASME*, vol. 67-DE-57, pp. 1–12, 1967.
- [2] J.O. Brooks, I.D. Walker, K.E. Green, J. Manganelli, J. Merino, L. Smolentzov, T. Threath, and P.M. Yanik, Robot Bedside Environments for Healthcare, *Proceedings 11<sup>th</sup> WSEAS International Conference on Signal Processing, Robotics, and Automation*, Cambridge, UK, February 2012, pp. 32-37.
- [3] R. Buckingham, Snake Arm Robots, *Industrial Robot: An International Journal*, vol. 29, no. 3, pp. 242-245, 2002.
- [4] R. Cieslak and A. Morecki, Elephant Trunk Type Elastic Manipulator – A Tool for Bulk and Liquid Type Materials Transportation, *Robotica*, vol. 17, pp. 11-16, 1999.
- [5] A. Grzesiak, R. Becker, and A. Verl, The Bionic Handling Assistant – A Success Story of Additive Manufacturing, *Assembly Automation*, Vol. 31, No. 4, 2011.
- [6] E. Guglielmino, N. Tsagarakis, and D.G. Caldwell, An Octopus-anatomy Inspired Robotics Arm, *Proceedings IEEE/RSJ International Conference on Intelligent Robots and Systems*, Taipei, pp 3091-3096, 2010.
- [7] M.W. Hannan and I.D. Walker, Analysis and Experiments with an Elephant’s Trunk Robot, *Advanced Robotics*, Vol. 15, No. 8, pp. 847-858, 2001.
- [8] S. Hirose, *Biologically Inspired Robots*: Oxford University Press, 1993.
- [9] G. Immega and K. Antonelli, The KSI Tentacle Manipulator, *Proceedings IEEE International Conference on Robotics and Automation*, Nagoya, Japan, pp. 3149-3154, 1995.
- [10] B. A. Jones, W. McMahan, and I. D. Walker, Design and Analysis of a Novel Pneumatic Manipulator, *Proc. 3rd IFAC Symposium on Mechatronic Systems*, Sydney, Australia, pp. 745–750, 2004.
- [11] A.D. Kapadia, I.D. Walker, D.M. Dawson, and E. Tatlicioglu, A Model-Based Sliding Mode Controller for Extensible Continuum Robots, *Proceedings 9<sup>th</sup> WSEAS International Conference on Signal Processing, Robotics, and Automation*, Cambridge, UK, February 2010, pp. 113-120.
- [12] W.M. Kier and K.K. Smith, Tongues, Tentacles and Trunks: The Biomechanics of Movement in Muscular-Hydrostats, *Zoological Journal of the Linnean Society*, Vol. 83, pp 307-324, 1985.
- [13] D. M. Lane, J. B. C. Davies, G. Robinson, D. J. O’Brien, J. Sneddon, E. Seaton, and A. Elfstrom, The AMADEUS Dextrous Subsea Hand: Design, Modeling, and Sensor Processing, *IEEE Journal of Oceanic Engineering*, vol. 24, no. 1, pp. 96-111, Jan. 1999.
- [14] W. McMahan, B. A. Jones, I. D. Walker, V. Chitrakaran, A. Seshadri, and D. Dawson, Robotic Manipulators Inspired by Cephalopod Limbs, *Proceedings of the CDEN Design Conference*, Montreal, Canada, pp. 1-10, 2004.
- [15] W. McMahan, B. A. Jones, and I. D. Walker, Design and Implementation of a Multi-section Continuum Robot: Air-Octor, *Proceedings IEEE/RSJ International Conference on Intelligent Robots and Systems*, Edmonton, Canada, pp. 3345-3352, 2005.
- [16] W. McMahan, M. Pritts, V. Chitrakaran, D. Dienno, M. Grissom, B. Jones, M. Csencsits, C.D. Rahn, D. Dawson, and I.D. Walker, Field Trials and Testing of “OCTARM” Continuum Robots, *Proceedings IEEE International Conference on Robotics and Automation*, pp. 2336-2341, 2006.
- [17] M. B. Pritts and C. D. Rahn, Design of an Artificial Muscle Continuum Robot, *Proceedings IEEE International Conference on Robotics and Automation*, New Orleans, Louisiana, pp. 4742-4746, 2004.
- [18] G. Robinson and J. B. C. Davies, Continuum Robots - A State of the Art, *Proceedings IEEE International Conference on Robotics and Automation*, Detroit, Michigan, pp. 2849-2854, 1999.
- [19] K. Suzumori, S. Iikura, and H. Tanaka, Development of Flexible Microactuator and its Applications to Robotic Mechanisms, *Proceedings IEEE International Conference on Robotics and Automation*, Sacramento, California, pp. 1622-1627, 1991.
- [20] D. Trivedi, C.D. Rahn, W.M. Kier, and I.D. Walker, Soft Robotics: Biological Inspiration, State of the Art, and Future Research, *Applied Bionics and Biomechanics*, 5(2), pp. 99-117, 2008.
- [21] H. Tsukagoshi, A. Kitagawa, and M. Segawa, Active Hose: An Artificial Elephant’s Nose with Maneuverability for Rescue Operation, *Proceedings IEEE International Conference on Robotics and Automation*, Seoul, Korea, pp. 2454-2459, 2001.
- [22] I.D. Walker, D. Dawson, T. Flash, F. Grasso, R. Hanlon, B. Hochner, W.M. Kier, C. Pagano, C.D. Rahn, Q. Zhang, Continuum Robot Arms Inspired by Cephalopods, *Proceedings SPIE Conference on Unmanned Ground Vehicle Technology VII*, Orlando, FL, pp 303-314, 2005.
- [23] R.J. Webster III and B.A. Jones, Design and Kinematic Modeling of Constant Curvature Continuum Robots: A Review, *International Journal of Robotics Research*, Vol. 29, No. 13, pp 1661-1683, November 2010.
- [24] S. Wakimoto and K. Suzumori, Fabrication and Basic Experiments of Pneumatic Multi-Chamber Rubber Tube Actuator for Assisting Colonoscope Insertion, *Proceedings IEEE International Conference on Robotics and Automation*, Anchorage, AK, pp 3260-3265, 2010.
- [25] P.M. Yanik, J. Manganelli, L. Smolentzov, J. Merino, I.D. Walker, J.O. Brooks, and K.E. Green, Toward Active Sensor Placement for Activity Recognition, *Proceedings 10<sup>th</sup> WSEAS International Conference on Signal Processing, Robotics, and Automation*, Cambridge, UK, February 2011, pp. 231-236.
- [26] A. Bartow, A. Kapadia, and I.D. Walker, A Novel Continuum Trunk Robot Based on Contractor Muscles, *Proceedings 12<sup>th</sup> WSEAS*

*International Conference on Signal Processing, Robotics, and Automation*, Cambridge, UK, February 2013, pp. 181-186.

- [27] I.D. Walker, "Impact Configurations and Measures for Kinematically Redundant and Multiple Armed Robot Systems", *IEEE Transactions on Robotics and Automation*, Vol. RA-10, #5, October 1994, pp. 670-683.
- [28] I.D. Walker, "Continuous Backbone "Continuum" Robot Manipulators: A Review", *ISRN Robotics*, Vol. 2013, July 2013, pp. 1-19.